Hindawi
Advances in Condensed Matter Physics
Volume 2022, Article ID 3233252, 7 pages
https://doi.org/10.1155/2022/3233252

Research Article

An Effective Route for the Growth of Multilayer MoS_2 by Combining Chemical Vapor Deposition and Wet Chemistry

Ziyad M. Almohaimeed,[1] **Shumaila Karamat**,[2] **Rizwan Akram**,[1] **Saira Sarwar**,[2] **Asad Javaid**,[2] **and Ahmet Oral**[3]

[1]*Department of Electrical Engineering, College of Engineering, Qassim University, P. O. Box 6677, Buraydah 51452, Saudi Arabia*
[2]*Laser Spectroscopy and Materials Synthesis Laboratory, Department of Physics, COMSATS University, Islamabad 54000, Pakistan*
[3]*Department of Physics, Middle East Technical University, Ankara 06800, Turkey*

Correspondence should be addressed to Ziyad M. Almohaimeed; z.mohaimeed@qu.edu.sa

Received 9 September 2021; Revised 6 January 2022; Accepted 8 January 2022; Published 9 February 2022

Academic Editor: Da-Ren Hang

Molybdenum disulfide (MoS_2) is an actively pursuing material of the 2D family due to its semiconducting characteristics, making it a potential candidate for nano and optoelectronics application. MoS_2 growth from molybdenum and sulphur precursors by chemical vapor depositions (CVD) is used widely, but molybdates' conversion into MoS_2 via CVD is overlooked previously. Direct growth of MoS_2 on the desired pattern not only reduces the interfacial defects but also reduces the complexities in device fabrication. In this work, we combine the wet synthesis and chemical vapor deposition method where sodium molybdate and L-cysteine are used to make a solution. With the dip coating, the mixture is coated on the substrates, and then, chemical vapor deposition is used to convert the chemicals into MoS_2. Raman spectroscopy revealed the presence of oxysulphides (peaks number value) other than A_{1g} and E^1_{2g}, where heat treatment was performed in the presence of Ar gas flow only. On the other hand, the films reducing in the presence of sulphur and argon gas promote only A_{1g} and E^1_{2g} peaks of MoS_2, which confirms complete transformation. XRD diffraction showed a very small change in the diffraction peaks and value of strain, whereas SEM imaging showed the flakes formation for MoS_2 samples which were heated in the presence of sulphur. X-ray photoelectron spectroscopy is also performed for the chemical composition and to understand the valence state of Mo, S, and O and other species.

1. Introduction

Transition metal dichalcogenides (TMDs) garner attention due to their potential in practical applications [1–6]. The physical and electronic properties of these 2D layered materials gave them credit for an exceptional class of materials. Photonics [4, 5], energy storage [7], sensing [8], electronic and optoelectronic [9, 10], lubrication and catalysis [11–14], and many other devices of TMDs showed remarkable results. Different chemical compositions of TMDs exhibit a semiconducting, semimetal, and superconducting behavior. Van der Waals forces stack covalently bound MoS_2 (S-Mo-S) in binary MX_2-layered materials [15]. In bulk form, it has an indirect band gap of 1.2 eV, which increases as the number of layers decreases due to the quantum confinement effect, reaching direct 1.9 eV band gap for the MoS_2 monolayer [16]. It is an indirect band gap semiconductor with a band gap energy of 1.2 eV in bulk form. Moreover, it exhibits mobility up to 200 cm^2/Vs [9], melting temperature greater than 1000°C [17], and room temperature stability for a longer duration [18], making it an ideal material for efficient device applications.

Various top-down approaches such as mechanical (scotch tape) and chemical (sonication) exfoliations have been used to synthesize MoS_2 [19–21]. Molecular defects, flake size, and control on layers number are not good in top-down approaches, which promote the low performance of electronic devices. To overcome these problems, various

bottom-up approaches such as physical vapor deposition [22, 23], chemical vapor deposition [24], hydrothermal technique [25], thiosalts thermal decomposition [26], and solvothermalization [27] are used for the direct growth of MoS_2 layers on the desired substrate. These bottom-up methods used a variety of molybdenum salts. A few of them contain sulphur, and few are without sulphur content and require extra sulphur content during growth, mostly called sulphurization. In the bottom-up approaches, chemical vapor deposition is widely used for MoS_2 growth on inert substrates. Mostly, in CVD approach, molybdenum trioxide (MoO_3) is reacted with sulphur compounds in the gas phases and resides on the desired substrate, but the real understanding of chemical phenomena and optimization to obtain high-quality MoS_2 is complicated in it. In sulphuration, sulphur powder and H_2S gas usually have been used as a sulphur source, and their appropriate amount snub the formation oxysulphides. In the present work, both sources of sulphur have been utilized. Sulphur powder is added in the furnace to react with the coated sodium molybdate and L-cystein solution, while H_2S gas is formed as a byproduct of the reaction during heating which promotes formation of MoS_2. Raman spectroscopy confirms the formation of monolayer MoS_2 and oxysulphides peaks for the samples where sulphur source was not added in the chamber. XRD also showed extra peaks for the samples without sulphur content and a higher value of strain compared to the sample formed in the presence of sulphur.

2. Materials and Methods

In this approach, we prepared MoS_2 via the solution of L-cysteine ($C_6H_{12}N_2O_4S_2$) and sodium molybdate dihydrate ($H_4MoNa_2O_6$) in DI water. Sodium molybdate is used as the precursor of molybdenum, while L-cystine is a source of sulphur in the growth of MoS_2. 2 g of L-cystein, as shown in Figure 1, and 1 g of sodium molybdate was mixed into 50 ml DI water under continuous sonication for 30 minutes. After sonication, a homogenous mixture is obtained, as shown in Figure 1 (c).

The solution is dropped on the cleaned SiO_2/Si substrates (3 drops on each substrate using a micrometer pipette). After drop coating (Figure 1 (e)), the substrates were dried on a hot plate at 100°C for 15 minutes (Figure 1 (f)). After drying, the samples are transferred to the CVD chamber, where the substrate was kept in the tube centre.

Argon (Ar) gas is used as a biproduct carrying gas maintained at a flow rate of 60 sccm. The samples are heated at 680°C for 1 hour in the presence-absence of 0.08 gm of sulphur (Figure 2). During the heating process, H_2S gas is being released and react with the precursors. As a result, the MoS_2 layer is formed on the substrates. The chemical reaction that occurs during the heating is

$$\begin{aligned} HSCH_2CHNH_2COOH + H_2O &\longrightarrow CH_3COCOOH + H_2O + NH_3 + H_2S \\ Na_2MoO_6H_4 + 2H_2S &\longrightarrow MoS_2 + 2NaOH^- + 2H_2O + 2OH^- \end{aligned} \quad (1)$$

Sodium molybdate decomposes, H_2S reacts with different species such as Mo by-products and converts it into MoS_2 on substrate, and further reaction with sulphur powder placed at the edge of the furnace zone occurs to avoid oxysulphides. The furnace used is calibrated, and temperature profile was obtained. The temperature mentioned in the centre of furnace was 680°C, and at the start of heating zone where sulphur was kept, it was measured as 120°C. After 1 hour, the CVD furnace was stopped, and the samples cool down in the presence of Ar gas. The substrates after chemical deposition showed a colour zone present on the substrate, which indicates MoS_2 growth, which is further confirmed by different characterization techniques.

Various characterization tools are employed to understand the complexities of the thin films. The Shimazdu X-ray diffractometer is used for structural information of MoS_2 thin films.

Horiba, Jobin Yvon iHR 550 Raman spectroscopy setup is used to know the optical signatures, JEOL JSM scanning electron microscopy is used for surface morphology, and VG ESCALAB 220I-XL X-ray photoelectron spectroscopy is used to get information about chemical bonding of MoS_2 films.

3. Results and Discussion

Raman spectra of MoS_2 samples with and without a sulphur source are shown in Figure 3. MoS_2 exhibits two feature modes E^1_{2g} and A_{1g}; the characteristic peaks of MoS_2 (A_{1g} and E^1_{2g}) look to be due to Mo and S atoms vibrating out-of-plane and in-plane, respectively. In our samples, the Raman spectra revealed a high strength of these two modes. Identification of the number of layers is possible by using the frequency difference ($\Delta f = fA_{1g} - E^1_{2g}$) between the two peaks/modes. The thickness information of MoS_2 layers is correlated to frequency changes between E^1_{2g} and A_{1g} [19]. As shown in Figure 3, the E^1_{2g} and A_{1g} peaks for MoS_2 without sulphur were 383.5 and 408.7 cm^{-1}, respectively. Moreover, the peaks for MoS_2 with sulphur were 383.2 and 408.4 cm^{-1}. A 25.2 cm^{-1} difference in frequency between the two peaks implies multilayer growth of MoS_2. Although certain peaks indicating oxysulphides are present in the samples, A_{1g} and E^1_{2g} Raman modes have the same location and intensity ratios, indicating that the quality of both CVD materials is comparable.

In addition, several experiments are performed at different concentrations of sulphur, and the presence of oxysulphides is observed for lower concentration of sulphur

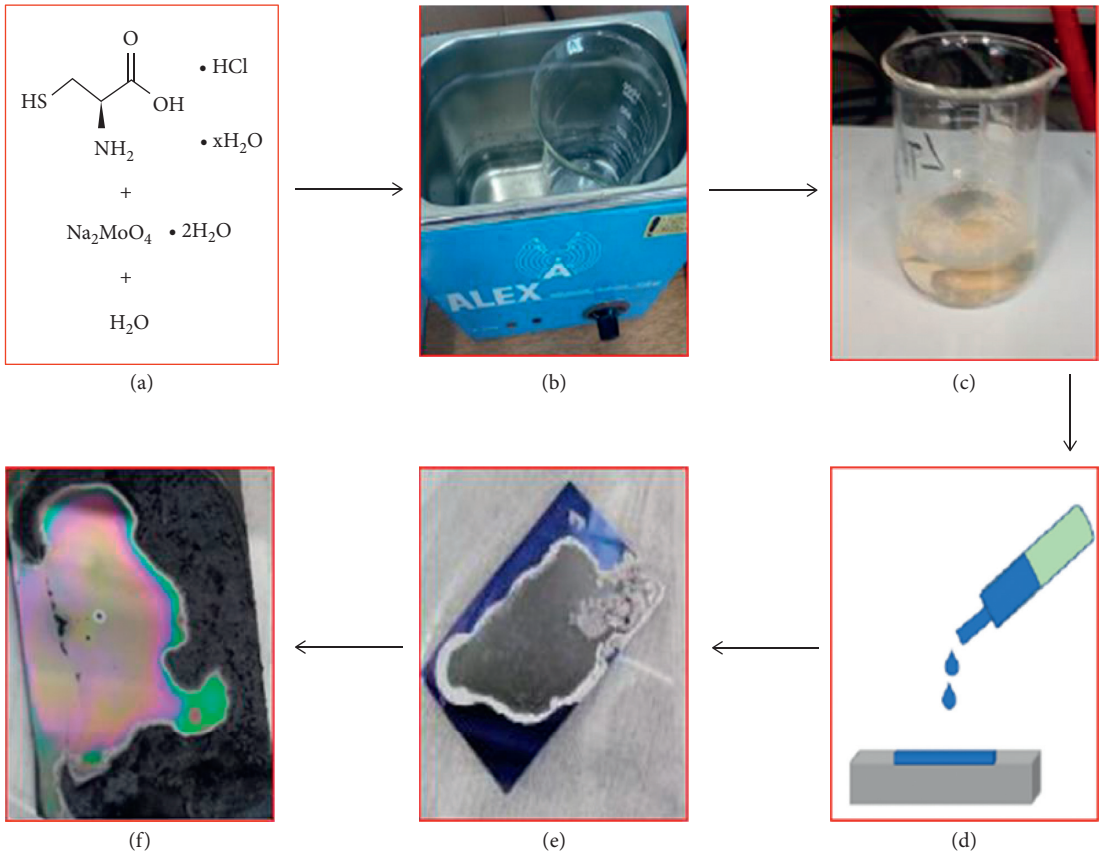

Figure 1: Schematic representation from solution formation to dip coating of samples.

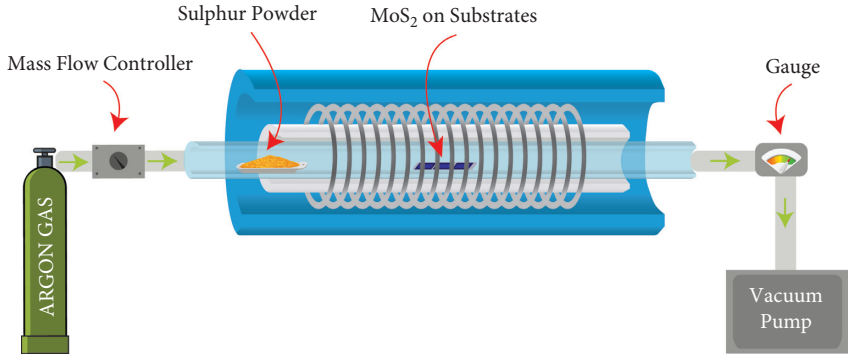

Figure 2: Schematic diagram of MoS_2 growth using the chemical vapor deposition (CVD) system.

such as 0.01 gm. Figure 4 shows the Raman spectrum of MoS_2 films sulphurated in the presence of 0.01 gm of sulphur. The presence of oxysulphides showed that the sulphur content is not enough to complete the reaction which results in peaks arising due to stretching and bending of Mo bonds with oxygen atoms. The ambient parameters are very important in the growth of 2D materials. For the applications of MoS_2, the presence of oxysulphides is not very encouraged, and sulphurisation is recommendable to remove sulphur-oxygen compounds arising due to shortage of sulphur.

CVD is a versatile technique for the growth of 2D materials [24, 28]. In Figure 5(a), the surface morphology of MoS_2 grown sample in the presence of sulphur clearly showed flakes-like structures arranged on top of each other. These flakes are multilayers that are arranged randomly on the substrate. During the conversion of MoS_2 layers, excessive sulphur content helps MoS_2 to aggregate. Whereas, MoS_2 grown without sulphur showed a rough sheet but not in the form of aggregated wide flakes (Figure 5(b)).

XRD pattern of MoS_2 matched with the Xpert high score database (JCPDS #00-037-1492) card. In Figure 6(a), MoS_2 in the presence of sulphur showed an intense peak of (002) at 14.8°, whereas the intensity of MoS_2 diffraction peak that appeared at (101) is less resembling the exact pattern of MoS_2. For the XRD of MoS_2 without sulphur content, the intensity of the (101) peaks enhance hints toward more

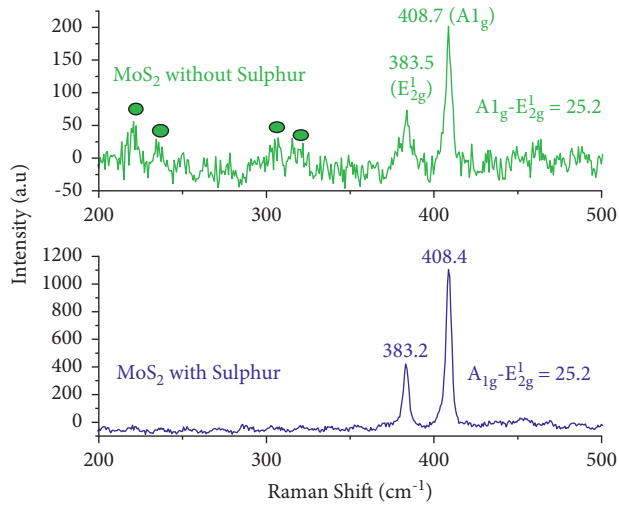

Figure 3: Raman spectrum of MoS_2 with and without sulphur confirming the growth of MoS_2.

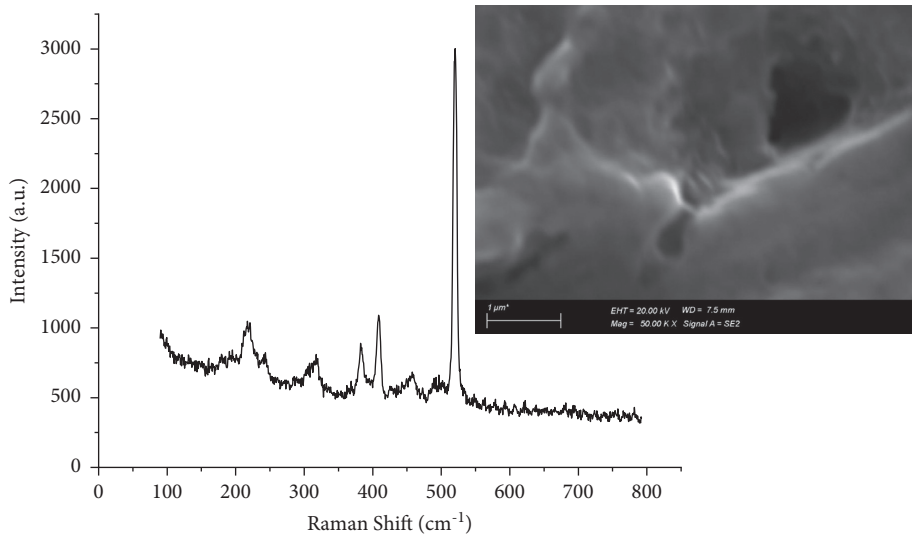

Figure 4: Raman spectrum of MoS_2 with (0.01 gm) sulphur confirming the growth of MoS_2 along with oxysulphides. Inset shows the surface morphology.

defects due to oxygen or oxysulphide information. Multiple diffraction peaks are obtained in MoS_2 samples, which showed polycrystalline nature.

Lattice strain was computed using Williamson–Hall (W-H) analysis and X-ray peak broadening analysis, assuming peak widths as a function of 2θ [29], where θ is Bragg's diffraction angle. The strain produced in powders as a result of crystal defects and deformations is estimated using lattice strain equation:

$$\frac{\Delta\xi}{\xi} = \frac{\beta}{\tan\theta}, \tag{2}$$

where β is the full-width half maximum (FWHM) of diffraction peak (in radian).

Lattice strain for the characteristic peak of (002) of MoS_2 with sulphur (Figure 6(a)) was calculated and found that it is displaced by lattice strain of 0.001, and for the other peak (101), it is displaced by 0.003. While (Figure 6(b)), XRD of MoS_2 without sulphur, lattice strain for the characteristic peak of (002) is calculated and found that it is displaced by lattice strain of 0.005, and for the other peak (101), it is displaced by 0.002. The lattice strain is higher for MoS_2 samples without sulphur content, which hints toward a higher defect state.

Because of the surface charge, there is a noticeable change in the C 1 s binding energy for MoS_2-generated samples in the C 1 s spectrum. Using the adventitious carbon C 1 s singlet (284.6 eV) as a reference, the binding energies of the elements were calibrated, as shown in Figure 7(a). For simplicity, we are presenting only the XPS spectra for the MoS_2 sample, which is grown in the presence of sulphur. The core peak spectra for Mo, S, and O were analyzed to see the interaction of these elements with each other. The core peaks of Mo and S both exhibited their doublets, with 3d3/2 and Mo 3d5/2 correlating to Mo 3d at 231.6 and 228.3 eV, respectively, and S_2p peaks as 2p3/2 and 2p1/2 at 161.2 and

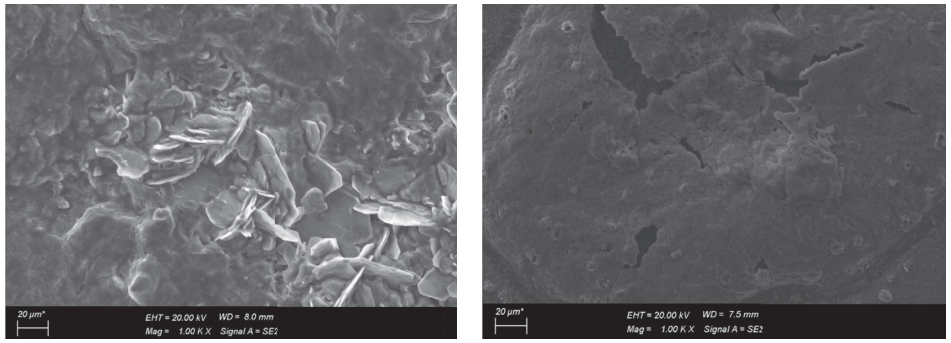

(a) (b)

Figure 5: (a) SEM image of MoS_2 with sulphur. (b) SEM image of MoS_2 without sulphur.

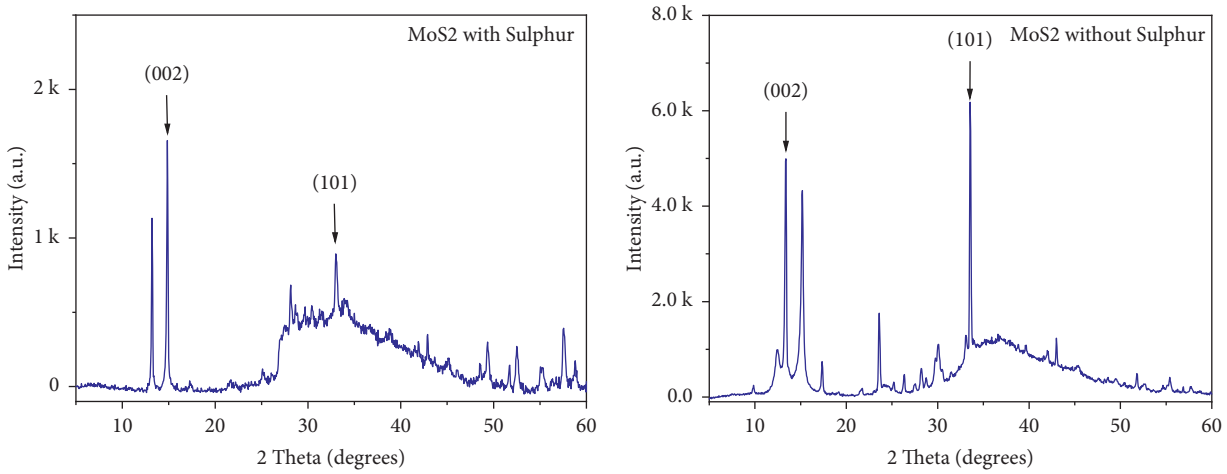

(a) (b)

Figure 6: XRD of MoS_2 (a) with sulphur and (b) without sulphur.

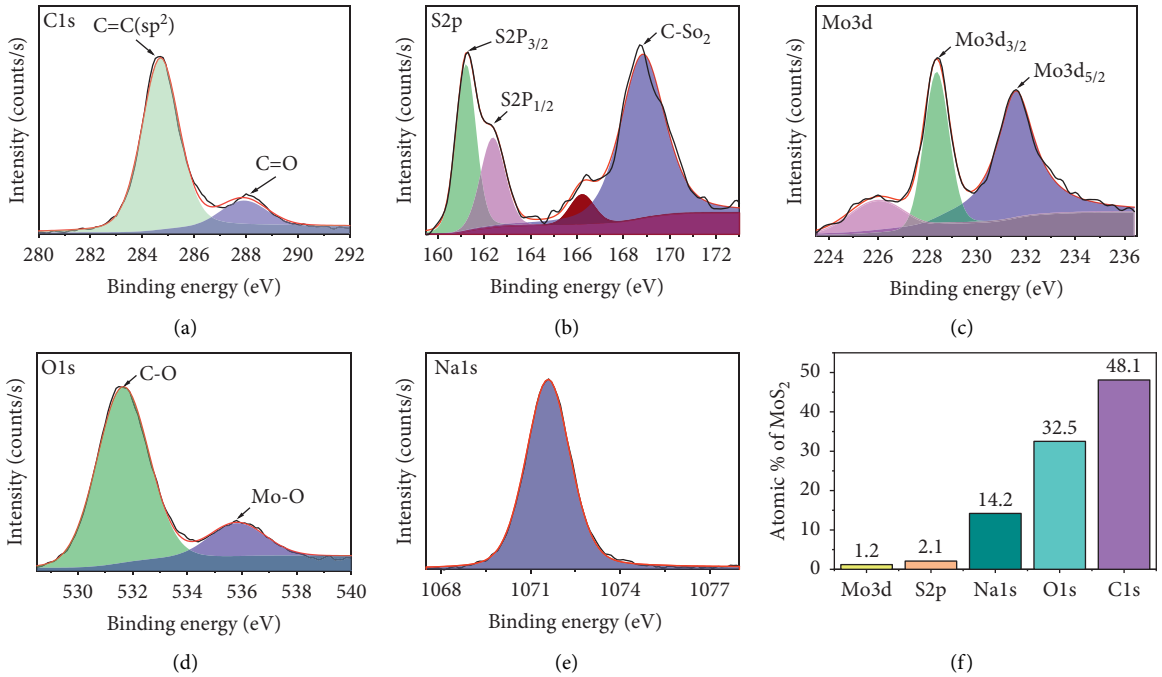

(a) (b) (c)

(d) (e) (f)

Figure 7: ((a)–(f)) XPS core peak spectrum of (a) C1s, (b) S_2P, (c) Mo_3d, (d) O1s, (e) Na, and (f) atomic percentage.

162.3 eV for S, respectively, as shown in Figures 7(b) and 7(c) [30]. The other peak that appeared at higher binding energy around 168.8 eV represents sulphate and carbon bonding. The binding energies of Mo and S represent the Mo + 4 and S-2 valence states. The occurrence of Mo and S doublets is a key feature seen in MoS_2 structures [31, 32], and their presence in our experimental finding supports the development of MoS_2 films. In addition to Mo +4 valence, Mo + 6 is also obtained in the sample, and Mo + 6 valence is enveloped by the broad peak of Mo 3d3/2 and Mo 3d5/2 (Figure 7(c)), which indicate that all the Mo-O bonds are not broken, and the transitions from the higher valence to lower valence of Mo maybe a temperature-dependent effect as observed by Salazar et al. [33]. In addition, the observed binding energy values for Mo bonds in our samples are also reported as the interaction of Mo with other elements [34]. Moreover, the presence of sulphur in the environment also facilitates the breaking of bonds between oxygen and molybdenum. Two main peaks were identified in the O 1s spectra of MoS_2 grown sample at 531.6 and 535.4.0 eV, and the peak at 535.4 eV suggests that Mo species and other oxidized compounds had complex oxygen bonding [26]. Deconvolution of the smaller doublets of Mo 3d enveloped in a broad peak at 226.4 eV also supports intermediate states of MoS_2, which occur owing to nonstoichiometric MoS_2 [35], as shown in the Raman spectra of samples. O 1 s peak is supposed to appear at 530 eV; but in our case, it is enveloped by the broad peak that appeared at 531.6 eV, as shown in Figure 7(d). The presence of other radicals on the surface is the cause of this broadening in the O 1 s spectrum. Sodium peak is also observed in the samples which showed some Na residues coming from precursor of sodium molybdate, as shown in Figure 7(e). Figure 7(f) shows the atomic percentage of all the elements present in our samples.

4. Conclusions

The present work is based on the combination of wet chemistry and the CVD growth method to synthesize MoS_2. Direct conversion of MoS_2 from liquid precursor under Ar flow at high temperature enables the conversion of L-cysteine and sodium molybdate solution-coated sample to convert into MoS_2. The effect of heating in the sulphur and nonsulphur environment is analyzed with the help of Raman and XRD analysis. Raman spectrum showed the presence of extra peaks of oxysulphides for the sample, which has no sulphur content. XRD peaks showed a slightly higher strain value for the samples with no sulphur than the samples with sulphur. SEM showed the formation of multilayer flakes for the MoS_2 samples formed in the presence of sulphur. Furthermore, XPS provides extensive information on the presence of various components in the samples. We successfully formed MoS_2 thin films by combining the wet chemistry and CVD method, which is confirmed by employing various characterizations. This method showed sulphurisation as an effective step to obtain good quality MoS_2 which would help design sensors where direct deposition of MoS_2 is required. However, few more experiments are still required to explore it further.

Data Availability

The data used to support the findings of this study are included within the article and are available from the corresponding author upon request.

Conflicts of Interest

The authors declare that they have no conflicts of interest.

Acknowledgments

The authors gratefully acknowledge Qassim University, represented by the Deanship of Scientific Research, on the financial support for this research under the number 10275-qec-2020-1-3-I during the academic year 1441 AH/2020 AD.

References

[1] X. Qian, J. Liu, L. Fu, and J. Li, "Quantum spin hall effect in two-dimensional transition metal dichalcogenides," *Science*, vol. 346, no. 6215, pp. 1344–1347, 2014.

[2] Y. Sun, S.-C. Wu, M. N. Ali, C. Felser, and B. Yan, "Prediction of Weyl semimetal in orthorhombic $MoTe_2$," *Physical Review B*, vol. 92, no. 16, Article ID 161107, 2015.

[3] J. T. Ye, Y. J. Zhang, R. Akashi, M. S. Bahramy, R. Arita, and Y. Iwasa, "Superconducting dome in a gate-tuned band insulator," *Science*, vol. 338, no. 6111, pp. 1193–1196, 2012.

[4] K. F. Mak and J. Shan, "Photonics and optoelectronics of 2D semiconductor transition metal dichalcogenides," *Nature Photonics*, vol. 10, no. 4, pp. 216–226, 2016.

[5] F. Xia, H. Wang, D. Xiao, M. Dubey, and A. Ramasubramaniam, "Two-dimensional material nanophotonics," *Nature Photonics*, vol. 8, no. 12, pp. 899–907, 2014.

[6] O. Lopez-sanchez, D. Lembke, M. Kayci, A. Radenovic, and A. Kis, "Ultrasensitive photodetectors based on monolayer MoS_2," *Nature Nanotechnology*, vol. 8, no. 7, pp. 497–501, 2013.

[7] Y. Sun, S. Gao, and Y. Xie, "Atomically-thick two-dimensional crystals: electronic structure regulation and energy device construction," *Chemical Society Reviews*, vol. 43, no. 2, pp. 530–546, 2014.

[8] F. K. Perkins, A. L. Friedman, E. Cobas, P. M. Campbell, G. G. Jernigan, and B. T. Jonker, "Chemical vapor sensing with monolayer MoS_2," *Nano Letters*, vol. 13, no. 2, pp. 668–673, 2013.

[9] B. Radisavljevic, A. Radenovic, J. Brivio, V. Giacometti, and A. Kis, "Single-layer MoS_2 transistors," *Nature Nanotechnology*, vol. 6, no. 3, pp. 147–150, 2011.

[10] K. Roy, M. Padmanabhan, S. Goswami et al., "Graphene-MoS_2 hybrid structures for multifunctional photoresponsive memory devices," *Nature Nanotechnology*, vol. 8, no. 11, pp. 826–830, 2013.

[11] Q. Fu, L. Yang, W. Wang et al., "Synthesis and enhanced electrochemical catalytic performance of monolayer WS2(1-x) Se2x with a tunable band gap," *Advanced Materials*, vol. 2, pp. 1–7, 2015.

[12] M. Asadi, K. Kim, C. Liu et al., "Nanostructured transition metal dichalcogenide electrocatalysts for CO_2 reduction in ionic liquid," *Science (New York, N.Y.)*, vol. 353, pp. 467–470, 2016.

[13] X. Zhou, D. Wu, H. Shi et al., "Study on the tribological properties of surfactant-modified MoS_2 micrometer spheres as an additive in liquid paraffin," *Tribology International*, vol. 40, no. 5, pp. 863–868, 2007.

[14] L. Rapoport, N. Fleischer, and R. Tenne, "Applications of $WS_2(MoS_2)$ inorganic nanotubes and fullerene-like nanoparticles for solid lubrication and for structural nanocomposites," *Journal of Materials Chemistry*, vol. 15, no. 18, pp. 1782–1788, 2005.

[15] G. Eda, H. Yamaguchi, D. Voiry, T. Fujita, M. Chen, and M. Chhowalla, "Photoluminescence from chemically exfoliated MoS_2," *Nano Letters*, vol. 11, no. 12, pp. 5111–5116, 2011.

[16] E. P. Nguyen, B. J. Carey, J. Z. Ou et al., "Electronic tuning of 2D MoS_2 through surface functionalization," *Advanced Materials*, vol. 27, no. 40, pp. 6225–6229, 2015.

[17] S. K. Singh, M. Neek-Amal, S. Costamagna, and F. M. Peeters, "Rippling, buckling, and melting of single- and multilayer MoS_2," *Physical Review B*, vol. 91, Article ID 014101, 2015.

[18] S. Kc, R. C. Longo, R. M. Wallace, and K. Cho, "Surface oxidation energetics and kinetics on MoS2 monolayer," *Journal of Applied Physics (Melville, NY, USA)*, vol. 117, Article ID 135301, 2015.

[19] H. Li, J. Wu, Z. Yin, and H. Zhang, "Preparation and applications of mechanically exfoliated single-layer and multilayer MoS2 and WSe2 nanosheets," *Accounts of Chemical Research*, vol. 47, no. 4, pp. 1067–1075, 2014.

[20] J. N. Coleman, M. Lotya, A. O'Neill et al., "Two-Dimensional nanosheets produced by liquid exfoliation of layered materials," *Science*, vol. 331, no. 6017, pp. 568–571, 2011.

[21] A. O'Neill, U. Khan, and J. N. Coleman, "Preparation of high concentration dispersions of exfoliated MoS_2 with increased flake size," *Chemistry of Materials*, vol. 24, pp. 2414–2421, 2012.

[22] J. V. Lauritsen, J. Kibsgaard, S. Helveg et al., "Size-dependent structure of MoS2 nanocrystals," *Nature Nanotechnology*, vol. 2, no. 1, pp. 53–58, 2007.

[23] S. S. Grønborg, S. Ulstrup, M. Bianchi et al., "Synthesis of epitaxial single-layer MoS_2 on Au(111)," *Langmuir*, vol. 31, pp. 9700–9706, 2015.

[24] Y.-H. Lee, X.-Q. Zhang, W. Zhang et al., "Synthesis of large-area MoS_2 atomic layers with chemical vapor deposition," *Advanced Materials*, vol. 24, no. 17, pp. 2320–2325, 2012.

[25] Y. Peng, Z. Meng, C. Zhong et al., "Hydrothermal synthesis and characterization of single-molecular-layer MoS_2 and $MoSe_2$," *Chemistry Letters*, vol. 30, no. 8, pp. 772-773, 2001.

[26] K.-K. Liu, W. Zhang, Y.-H. Lee et al., "Growth of large-area and highly crystalline MoS_2 thin layers on insulating substrates," *Nano Letters*, vol. 12, no. 3, pp. 1538–1544, 2012.

[27] H. Du, D. Liu, M. Li, R. L. Al Otaibi, R. Lv, and Y. Zhang, "Solvothermal synthesis of MoS_2 nanospheres in DMF-water mixed solvents and their catalytic activity in hydrocracking of diphenylmethane," *RSC Advances*, vol. 5, no. 97, pp. 79724–79728, 2015.

[28] S. Chaitoglou, T. Giannakopoulou, T. Speliotis, A. Vavouliotis, C. Trapalis, and A. Dimoulas, "Mo_2C/Graphene heterostructures: low temperature chemical vapor deposition on liquid bimetallic Sn-Cu and hydrogen evolution reaction electrocatalytic properties," *Nanotechnology*, vol. 30, no. 12, Article ID 125401, 2019.

[29] A. Mishra, V. K. Singh, and T. Mohanty, "Coexistence of interfacial stress and charge transfer in graphene oxide-based magnetic nanocomposites," *Journal of Materials Science*, vol. 52, no. 13, pp. 7677–7687, 2017.

[30] N. Brown, N. Cui, and A. McKinley, "An XPS study of the surface modification of natural MoS_2 following treatment in an RF-oxygen plasma," *Applied Surface Science*, vol. 134, pp. 11–21, 1998.

[31] E. Buzaneva, T. Vdovenkova, A. Gorchinsky et al., "XPS and STS of layered semiconductor MoSx," *Journal of Electron Spectroscopy and Related Phenomena*, vol. 68, pp. 763–769, 1994.

[32] L. Benoist, D. Gonbeau, G. Pfister-Guillouzo, E. Schmidt, G. Meunier, and A. Levasseur, "X-ray photoelectron spectroscopy characterization of amorphous molybdenum oxysulfide thin films," *Thin Solid Films*, vol. 258, no. 1-2, pp. 110–114, 1995.

[33] N. Salazar, I. Beinik, and J. V. Lauritsen, "Single-layer MoS_2 formation by sulfidation of molybdenum oxides in different oxidation states on Au (111)," *Physical Chemistry Chemical Physics: PCCP*, vol. 19, pp. 14020–14029, Article ID 14020, 2017.

[34] C. Stefanos, G. Tatiana, P. George et al., "Cu vapor-assisted formation of nanostructured Mo_2C electrocatalysts via direct chemical conversion of Mo surface for efficient hydrogen evolution reaction applications," *Applied Surface Science*, vol. 510, Article ID 145516, 2020.

[35] S. Karamat, M. U. Hassan, J. S. Pan, L. Tabassam, and A. Oral, "Chemical vapor deposition of molybdenum disulphide on platinum foil," *Materials Chemistry and Physics*, vol. 249, Article ID 123017, 2020.